

A Genetic Map and Recombination Parameters of the Human Malaria Parasite *Plasmodium falciparum*

Xin-zhuan Su,¹ Michael T. Ferdig,¹ Yaming Huang,²
 Chuong Q. Huynh,³ Anna Liu,¹ Jingtao You,¹ John C. Wootton,³
 Thomas E. Wellems^{1*}

Genetic investigations of malaria require a genome-wide, high-resolution linkage map of *Plasmodium falciparum*. A genetic cross was used to construct such a map from 901 markers that fall into 14 inferred linkage groups corresponding to the 14 nuclear chromosomes. Meiotic crossover activity in the genome proved high (17 kilobases per centimorgan) and notably uniform over chromosome length. Gene conversion events and spontaneous microsatellite length changes were evident in the inheritance data. The markers, map, and recombination parameters are facilitating genome sequence assembly, localization of determinants for such traits as virulence and drug resistance, and genetic studies of parasite field populations.

The pressing need for progress against *P. falciparum* has led to international research initiatives, including collaborations to sequence the genome, determine its transcription patterns, and characterize its expressed gene products (1). In these efforts, genetic mapping and linkage analysis are essential to locate and verify monogenic and multi-genic determinants involved in traits of drug resistance (2, 3), transmission and gamete development (4), and virulence attributes that include parasite-mediated cytoadherence and host cell invasion (5, 6). Marker location data, together with information on recombination frequencies and patterns, further provide the basis for exploring genetic structure and variation in parasite populations (7).

For the genetic map reported here, we designed primer pairs for 1759 *P. falciparum* simple sequence repeats (8). More than 45% of these primer pairs provided distinguishable length differences between products amplified from the HB3 and Dd2 parents of a *P. falciparum* cross (2). These microsatellites were used in conjunction with a previous set of restriction fragment length polymorphism (RFLP) markers to establish inheritance for a

total of 901 markers in 35 independent progeny (9).

The 901 markers constitute an approximately uniform set with an average spacing of 30 kb, based on the *P. falciparum* genome size of 25,000 to 30,000 kb (6). These markers show expected patterns of haploid inheritance and fall within 14 inferred linkage groups, corresponding to the nuclear chromosomes of *P. falciparum* (Fig. 1) (10). Inheritance patterns within these 14 linkage groups distinguish 326 map segments, each defined by one or more markers, having an average length of 80 kb. The relative sizes of the linkage groups correlate closely with physical lengths of the chromosomes and span 1556 centimorgans (cM), indicating an average map unit distance of 17 kb/cM. This relation is uniform over the 14 parasite chromosomes (Fig. 2). The marker order in linkage groups 2 and 3 is congruent with recently reported sequences from the corresponding chromosomes (8).

Counts and locations of the crossovers are modeled well by a single Poisson process over almost all regions of the 14 linkage groups (Fig. 3) (11, 12). Compared with most eukaryotic systems, the *P. falciparum* genome thus has a high and unusually uniform meiotic crossover activity per physical length of DNA, with only a few intermarker intervals showing counts that might suggest more activity than expected for a strictly random process (13). Additional data will be required to determine whether these intervals result from atypical marker spacings or indicate recombination hotspots.

The analysis of the haplotypes in the HB3 × Dd2 cross provides evidence for mei-

otic gene conversion events in addition to the reciprocal crossovers. In 28 confirmed instances (Fig. 4), a single marker of one parental type was found flanked on both

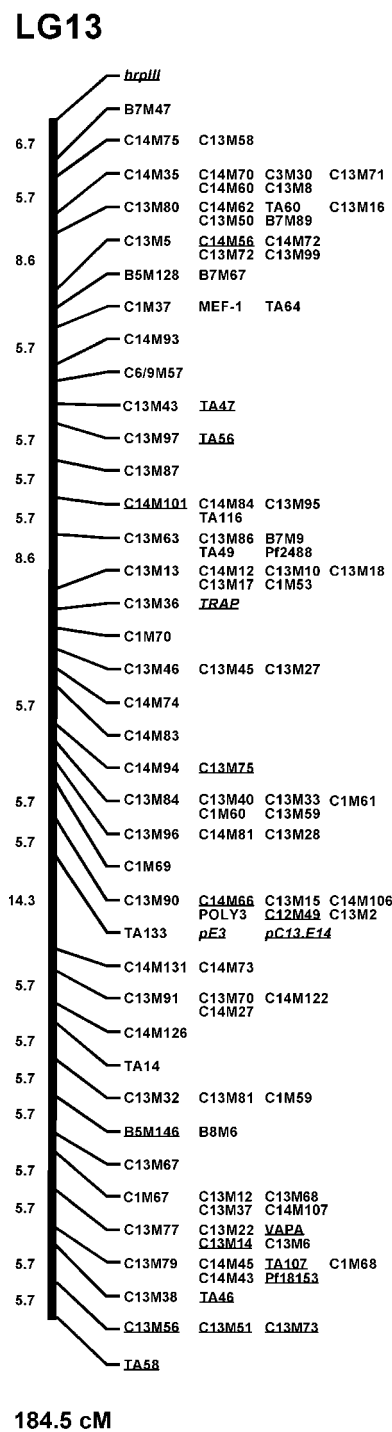


Fig. 1. Linkage map corresponding to *P. falciparum* chromosome 13. Markers confirmed by physical mapping are underlined. RFLP markers are indicated in italics. Only intermarker distances of more than 4 cM are labeled. Maps of linkage groups corresponding to the other chromosomes, segregation data, and marker and primer information are provided on the Internet (11).

¹Laboratory of Parasitic Diseases, National Institute of Allergy and Infectious Diseases, National Institutes of Health, Bethesda, MD 20892-0425, USA. ²Guangxi Institute of Parasitic Disease Control, 80 Taoyuan Road, Nanning, Guangxi 530021, Peoples' Republic of China. ³Computational Biology Branch, National Center for Biotechnology Information, National Library of Medicine, National Institutes of Health, Bethesda, MD 20894-6075, USA.

*To whom correspondence should be addressed. E-mail: tew@helix.nih.gov

REPORTS

Fig. 2. Plot of physical length versus number of observed crossovers in the 14 nuclear chromosomes of *P. falciparum*. The linear unweighted least squares regression line extrapolates to zero crossovers at zero physical length and has a slope of one crossover per 1.67×10^6 base pairs per inferred meiosis, in close agreement with the average value of 17 kb/cM for the entire genome. Chromosome sizes are from pulsed-field gel data (6).

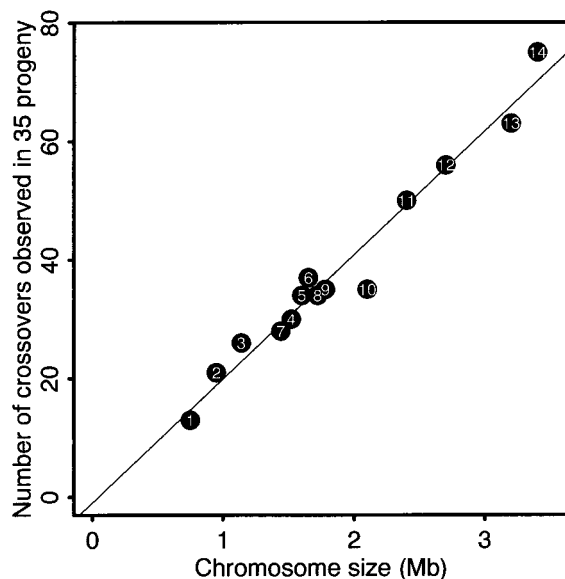


Fig. 3. Crossover counts, crossover locations, and genotype segregation proportions for the linkage group corresponding to *P. falciparum* chromosome 13. Data for other chromosomes are provided on the internet (11). Vertical bars show the crossover counts, and the plotted line indicates the proportion of Dd2 allele in the progeny. Dashed horizontal lines delimit the approximate 95% probability range for segregation. Positions of hrpIII (accession number U69552), MEF-1 (X60488), TRAP (X13022), RNA polymerase III (M73770), and VAPA (L08200) are indicated.

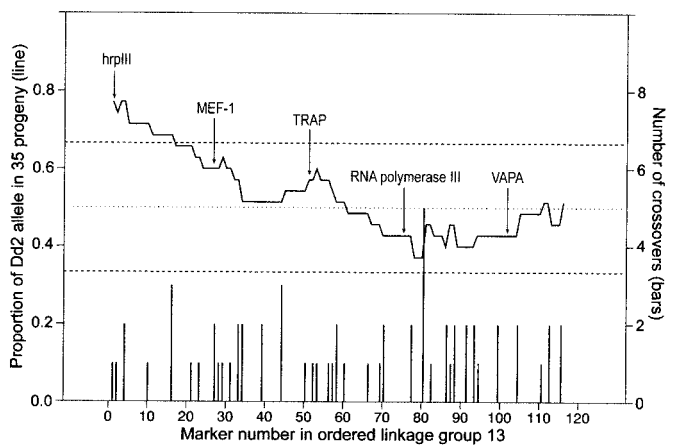
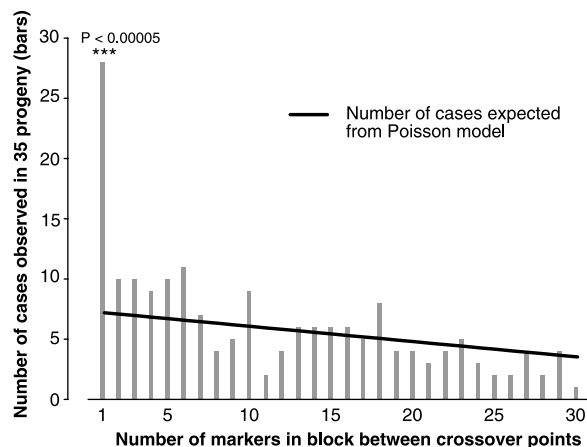


Fig. 4. Significant excess of single-marker events attributable to nonreciprocal conversion in the *P. falciparum* HB3 \times Dd2 cross. The horizontal axis indicates the number of markers, n , for any uninterrupted parental haplotype flanked on both sides by the other parental type [for example, the four D (Dd2) markers between flanking blocks of H (HB3) markers in the string HH-HHHHHHHHDDDDHHHHHHHH-HH represent a value of $n = 4$]. The vertical bars indicate the observed number for each value of n from 1 to 30. The plotted line represents the expected number calculated from the simple random model based on a single Poisson process (14). Haplotype strings are available from the segregation data (11).



sides by markers of the other parental type, significantly in excess of the 7.2 instances predicted on the basis of reciprocal crossovers

alone ($P < 0.00005$) (14). We attribute this excess to nonreciprocal conversions of short DNA segments, as is generally observed in

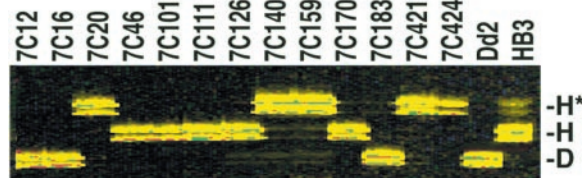
eukaryotic systems that resolve meiotic recombination intermediates through either crossover or nonreciprocal conversion configurations (15). Because DNA segments involved in such conversions are typically much less than the 30-kb average spacing in the map, many non-reciprocal events would be undetected by the current marker set.

For 13 microsatellite markers, spontaneous mutational events were evident in segregation patterns that showed a third allele different from either one of the two canonical parental alleles (Fig. 5). These third alleles were seen in multiple progeny for eight of the 901 markers and in only one of the progeny for another five markers (16). The third allele in each case was inherited exclusive of a corresponding canonical parental allele. Some of these mutational events had occurred within the clonal populations of parental erythrocytic stages, as the third microsatellite bands could be amplified as minor products from parental DNA (Fig. 5).

Although the large majority of the biallelic markers exhibited approximately equal numbers of parental forms in the progeny, segregation disparities were present in regions of seven linkage groups. Most of chromosome 2 and terminal regions of chromosomes 9 and 13 showed significant excesses of Dd2 markers; marginal excesses were also found in short segments of chromosomes 11 and 12 (Fig. 3) (11). Conversely, substantial regions of chromosomes 3 and 8 carried excesses of HB3 markers. Some of these regions include chromosome DNA rearrangements, such as deletion of the knob-related gene (KAHRP) from Dd2 chromosome 2 (9) and a subtelomeric translocation in HB3 chromosome 13 (17). Also, certain favored haplotypes may have been selected among the enhanced numbers of recombinant HB3 \times Dd2 oocysts that were observed in infected mosquitoes (9).

The *P. falciparum* linkage map, genome-wide availability of polymorphic markers, and recombination parameters are of value in several areas of field and laboratory research. The mapped, sequence-tagged markers currently provide a scaffold on which sequence assemblies from the *P. falciparum* genome project can be assigned to chromosomes, ordered, and oriented. Over the long term, the markers, mapping data, and information on recombination parameters will support laboratory genetic studies and the genome-wide tracing of chromosomal regions in parasite field samples. Linkage data from such work will provide fundamental information on disease determinants and on the genetic structure of *P. falciparum* populations in malarious regions.

Fig. 5. Evidence of a spontaneous microsatellite length change in the HB3 population detected by marker TA101. The upper band (H*) in the HB3 lane indicates the presence of a noncanonical allele in the parental population. Signals from the 7C20, 7C140, 7C159, 7C421, and 7C424 parasites show that this mutant allele was inherited exclusive of the canonical HB3 or Dd2 alleles (H, D).



References and Notes

1. D. Butler, *Nature* **388**, 701 (1997); E. Bond and M. J. F. Austin, *Science* **275**, 1051 (1997); T. E. Wellems, X. Su, M. Ferdig, D. A. Fidock, *Curr. Opin. Microbiol.* **2**, 415 (1999).
2. T. E. Wellems *et al.*, *Nature* **345**, 253 (1990); X. Su, L. A. Kirkman, H. Fujioka, T. E. Wellems, *Cell* **91**, 593 (1997).
3. P. Wang, M. Read, P. F. Sims, J. E. Hyde, *Mol. Microbiol.* **23**, 979 (1997).
4. A. B. Vaidya *et al.*, *Mol. Biochem. Parasitol.* **69**, 65 (1995); F. Guinet *et al.*, *J. Cell Biol.* **135**, 269 (1996).
5. K. P. Day *et al.*, *Proc. Natl. Acad. Sci. U.S.A.* **90**, 8292 (1993).
6. T. E. Wellems *et al.*, *Cell* **49**, 633 (1987).
7. R. E. L. Paul *et al.*, *Science* **269**, 1709 (1995).
8. Chromosomal DNAs were purified by pulsed-field gradient electrophoresis, cloned, and screened for simple sequence repeats by hybridization with ³²P-labeled (TAA)₁₀ and (T)₁₉ oligonucleotides [X. Su and T. E. Wellems, *Genomics* **33**, 430 (1996)]. Simple sequence repeats were also obtained from GenBank deposits and from the *P. falciparum* genome project, including data from recently reported sequences of chromosomes 2 and 3 [M. J. Gardner *et al.*, *Science* **282**, 1126 (1998); S. Bowman *et al.*, *Nature* **400**, 532 (1999); www.tigr.org/tdb/mdb/pfadb/pfdb.html; www.sanger.ac.uk/Projects/P_falciparum/; sequence-www.stanford.edu/group/malaria/index.html]. Fluorescent detection of microsatellites was according to X. Su, D. J. Carucci, and T. E. Wellems [*Exp. Parasitol.* **89**, 262 (1998)].
9. A. Walker-Jonah *et al.*, *Mol. Biochem. Parasitol.* **51**, 313 (1992). The 35 independent progeny were isolated from the set of HB3 × Dd2 clones described by L. A. Kirkman, X. Su, and T. E. Wellems [*Exp. Parasitol.* **83**, 147 (1996)].
10. Assignments and relative order of the markers were determined by the Mapmaker program [S. E. Lincoln and E. S. Lander, *Genomics* **14**, 604 (1992); E. S. Lander *et al.*, *Genomics* **1**, 174 (1987)]. Physical assignments of 154 markers were also established with chromosome DNAs separated by pulsed-field gradient electrophoresis.
11. The full segregation data set, marker data, and mapping information are available at www.ncbi.nlm.nih.gov/Malaria/index.html.
12. S. Karlin and U. Liberman, *Adv. Appl. Probab.* **11**, 479 (1979); U. Liberman, *J. Math. Biol.* **21**, 1 (1984). Poisson parameters were fitted to individual chromosomes as well as genome-wide crossover count distributions. Results were found to be consistent with a single count-location process, and generalized interference functions were not necessary to model the data.
13. Significant spikes of crossover activity were observed in chromosomes 12 and 9, whereas the elevation of counts seen near the RNA polymerase III gene in chromosome 13 (Fig. 3) is of marginal statistical significance ($P = 0.06$). A table comparing recombination frequencies in eukaryotic organisms is available at the National Center for Biotechnology Information web site (11).
14. The theoretical line was calculated from the distributions of the distances between pairs of random points occurring uniformly within a bounded interval. Fourteen individual computations were performed on the basis of the numbers of intermarker spaces in the 14 linkage groups. The model and its expected variance were confirmed by simulations. For the purpose of calculating map parameters, all single-marker

events ($n = 1$; Fig. 4) were classified as gene conversion candidates and were excluded from counts of crossovers. All other events ($n \geq 2$; Fig. 4) were classified as pairs of crossovers. Assignment errors in

this classification scheme would have produced negligible consequence on the overall analysis, as they are few and tend to cancel out.

15. P. J. Hastings, *Mutat. Res.* **284**, 97 (1992).
16. The eight markers with noncanonical alleles in multiple progeny are C3M29, TA101, C4M41, BM83, P11_1, CH12M29, C14M56, and C14M92; the other five markers are C4M76, C3M63, Y357M3, Y357M2.2, and TA88.
17. K. Hinterberg, D. Mattei, T. E. Wellems, A. Scherf, *EMBO J.* **13**, 4174 (1994).
18. We thank T. Tatusov for graphical display software; D. Severson and A. A. Schäffer for discussions on linkage analysis; and K. Pruitt, J. Ostell, and D. Lipman for advice and support. Y. Huang gratefully acknowledges sabbatical support from the China Scholarship Council.

12 July 1999; accepted 29 September 1999

Sexual Transmission and Propagation of SIV and HIV in Resting and Activated CD4⁺ T Cells

Z.-Q. Zhang,¹ T. Schuler,¹ M. Zupancic,¹ S. Wietgreffe,¹ K. A. Staskus,¹ K. A. Reimann,² T. A. Reinhart,³ M. Rogan,¹ W. Cavert,¹ C. J. Miller,⁴ R. S. Veazey,² D. Notermans,⁵ S. Little,⁶ S. A. Danner,⁵ D. D. Richman,^{6,10} D. Havlir,⁶ J. Wong,^{6,10} H. L. Jordan,² T. W. Schacker,⁷ P. Racz,⁸ K. Tenner-Racz,⁸ N. L. Letvin,² S. Wolinsky,⁹ A. T. Haase^{1*}

In sexual transmission of simian immunodeficiency virus, and early and later stages of human immunodeficiency virus–type 1 (HIV-1) infection, both viruses were found to replicate predominantly in CD4⁺ T cells at the portal of entry and in lymphoid tissues. Infection was propagated not only in activated and proliferating T cells but also, surprisingly, in resting T cells. The infected proliferating cells correspond to the short-lived population that produces the bulk of HIV-1. Most of the HIV-1–infected resting T cells persisted after antiretroviral therapy. Latently and chronically infected cells that may be derived from this population pose challenges to eradicating infection and developing an effective vaccine.

HIV-1 is usually transmitted by heterosexual contact (1) and, in prevailing hypothetical reconstructions of the initial events in infection, is believed to first infect dendritic cells (DCs) or

macrophages (Mφs) (2–11). At a later, undefined time these cell types pass infection to CD4⁺ T cells in postulated cell-cell interactions that activate the T cells so that they become susceptible to and can support virus replication (3, 11). We experimentally examined this reconstruction of heterosexual transmission in an animal model. We inoculated 14 rhesus monkeys (*Macaca mulatta*) intravaginally with uncloned simian immunodeficiency virus (SIV) monoclonal antibody mac251, a dual tropic strain that replicates in cultured Mφs or T cell lines (12, 13). To identify the types of cells in which SIV first replicates we euthanized animals 1, 3, 7, and 12 days after inoculation and looked in tissue sections by in situ hybridization (ISH) for cells with detectable SIV RNA (14, 15). In screening ≥ 25 sections of tissues from the site of inoculation and distal sites in the lymphatic and other organ systems, we first detected SIV RNA in a small number of cells 3 days after inoculation only in the endocervical

¹Department of Microbiology, University of Minnesota Medical School, Minneapolis, MN 55455, USA. ²Division of Viral Pathogenesis, Beth Israel Hospital, Harvard University, Boston, MA 02215, USA. ³Department of Infectious Diseases and Microbiology, University of Pittsburgh, Pittsburgh, PA 15261, USA. ⁴California Regional Primate Research Center, Davis, CA 95616, USA. ⁵Division of Infectious Diseases, Tropical Medicine and AIDS, Academic Hospital, University of Amsterdam, Academic Medical Centre, Amsterdam, 1105 AZ, Netherlands. ⁶Departments of Pathology and Medicine, University of California, San Diego, CA 92093, USA. ⁷Department of Medicine, University of Minnesota Medical School, Minneapolis, MN 55455, USA. ⁸Bernhard-Nocht Institute for Tropical Medicine, Hamburg 20359, Germany. ⁹Division of Infectious Disease, Northwestern University Medical School, Chicago, IL 60611, USA. ¹⁰San Diego VA Health Care System, San Diego, CA 92093, USA.

*To whom correspondence should be addressed.